Riv. Mat. Univ. Parma, Vol. **2** (2011), 57-76

A.-V. PHAN and V. GUDURU

Boundary element transient analysis of the dynamic *T*-stress and biaxiality ratio

Abstract. In this paper, we introduce a 2-D boundary integral equation (BIE) for determining the *T*-stress for cracks under dynamic loading conditions (dynamic *T*-stress or DTS). This BIE is only weakly singular and it can be used in the post-processing stage of a boundary element dynamic analysis of cracks. The formula can also be employed, in conjunction with any technique for the mode-I dynamic stress intensity (DSIF), for calculating the dynamic biaxiality ratio (DBR). In this work, the proposed BIE is formulated in the frequency domain so it can be used within the framework of the symmetric-Galerkin boundary element method for elastodynamics in the Fourier-space frequency domain. By applying the inverse fast Fourier transform to the frequency responses of the DTS and mode-I DSIF, the time histories (transient responses) of the DTS and DBR can be obtained. Numerical examples involving 2-D crack plates subjected to the Heaviside step loading are presented. The DTS results obtained from the aforementioned BIE are compared with some references available in the literature to validate the proposed technique.

Keywords. Dynamic *T*-stress, dynamic biaxiality ratio, symmetric-Galerkin boundary element method, elastodynamics, frequency analysis, transient responses.

Mathematics Subject Classification (2000): 65N38, 74R10.

1 - Introduction

In classical theories of fracture mechanics, the stress and displacement fields in the vicinity of a crack tip are characterized by a single parameter called the stress intensity factor (SIF). However, numerous experimental work (*e.g.*, [**1, 2**]) have

Received: April 1, 2010; accepted: May 7, 2010.

shown that a second fracture parameter, known as the elastic T-stress (the first non-singular term in the series expansion of the stress component parallel to the crack and ahead of a crack tip) plays an important role in the linear elastic fracture mechanics of brittle materials under mixed-mode loading conditions. As a result, there has been increasing attempts to describe the crack tip behavior in terms of both the SIF and T-stress, and a larger and larger amount of investigation has been devoted to the numerical evaluation of the T-stress. For example, finite element method (FEM, *e.g.*, [**3, 4**]), boundary element method (BEM, *e.g.*, [**5, 6**]), symmetric-Galerkin BEM (SGBEM, *e.g.*, [**7**]), complex variable function method [**8**], *etc.*, have been employed to calculate the elastostatic T-stress. Generally, the numerical techniques developed for determining the T-stress can be classified into three groups [**5**]: the methods based upon inspection of the numerical solution, the path-independent interaction M-integral method, and the second-order weight function method.

As the use of composite materials in industry (*e.g.*, airframes) has expanded, there is a special interest in their fracture behavior under impact loading conditions. This has motivated many studies on the dynamic SIFs (DSIFs) and dynamic T-stress (DTS). However, while there is a large number of numerical investigations for the DSIFs (*e.g.*, [**9, 10, 11, 12, 13, 14, 15, 16, 17**]), the situation is less encouraging for the DTS. Only a few studies on the DTS can be found in the literature such as those using BEM by Sladek *et al.* [**18**], FEM by Jayadevan *et al.* [**19, 20**], and scaled boundary FEM (SBFEM) by Song and Vrcelj [**21**]. It is important to note that most of these DTS calculations ([**18, 19, 20**]) are based upon the interaction integral (or M-integral) method.

Although the T-stress and DTS can be computed directly from the asymptotic expansion [**22**] for the crack-tip stress field, there was a concern over the fact that the numerical result was sensitive to the distance from the crack tip to a point selected for calculating the T-stress or DTS [**18**] (concern over the singularity of the numerical result if the T-stress or DTS are evaluated at the crack-tip location). However, as demonstrated in [**6**], a non-singular boundary integral equation (BIE) can be derived using the asymptotic stress expansion and thus, the T-stress can be directly computed at the crack-tip location. A similar technique is proposed in this paper to derive a weakly singular 2-D BIE in the Fourier-space frequency domain for determining the DTS. This BIE is general and it can be employed as a post-processing step in any version of the frequency-domain boundary element analysis. Within this work, the SGBEM for elastodynamics in the Fourier-space frequency domain is the version of choice.

As frequency-domain analysis is employed in this work, the DTS produced from a SGBEM analysis is a function of frequency. If a time history (transient response) of the DTS is needed, fast Fourier transform (FFT) and inverse FFT (IFFT) can be used to obtain the time-dependent quantity.

By normalizing the T-stress relative to the mode-I SIF (K_{I}), Leevers and Radon [**23**] proposed a dimensionless parameter called the biaxiality ratio B. Although this is a preferred choice for normalizing the T-stress or DTS, the accuracy of B depends on that of both the T-stress and K_{I}. Motivated by the accuracy of the proposed BIE for numerically evaluating the DTS and that of the technique using the modified quarter-point (MQP) element for computing the DSIFs reported in [**16, 17**], the computation of the dynamic biaxiality ratio (DBR) is also a subject of this paper.

Four test examples are presented to demonstrate the accuracy and effectiveness of using the proposed BIE in evaluating the DTS and DBR for two cracked plates subjected to an impact loading in the form of the Heaviside step function $H(t)$ where t is time.

2 - Elastodynamic SGBEM for fracture analysis in the Fourier-space frequency domain

A review of the elastodynamic SGBEM is given in this section as the proposed BIE for evaluating the DTS is implemented as a post-processing step of a fracture analysis using this method.

2.1 - *Symmetric-Galerkin formulation*

Consider a finite domain containing a crack composed of two surfaces Γ_c^+ and Γ_c^- symmetrically loaded as shown in Fig. 1. Let the boundary of the domain be Γ and $\Gamma = \Gamma_b \cup \Gamma_c^+ \cup \Gamma_c^-$. Also, let the non-crack boundary $\Gamma_b = \Gamma_{bu} \cup \Gamma_{bt}$ where Γ_{bu} is part of Γ_b where displacement is specified and Γ_{bt} is part of Γ_b where traction is prescribed. Finally, let $\Gamma_t = \Gamma_{bt} + \Gamma_c^+$ and note that traction is supposed to be known on $\Gamma_c = \Gamma_c^+ \cup \Gamma_c^-$.

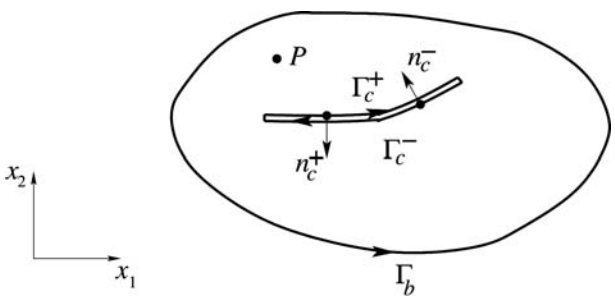

Fig. 1. A domain containing a crack.

The Navier-Cauchy governing equation for elastodynamics without body force is given by

$$(c_p^2 - c_s^2)u_{i,ij}(Q,t) + c_s^2 u_{j,ii}(Q,t) - \ddot{u}_j(Q,t) = 0 \tag{1}$$

where commas and dots denote space and time differentiations, respectively, and $u_i(Q,t)$ represents the displacement vector at a field point Q and at time t. The compressional (c_p) and shear (c_s) velocities are known to be

$$c_p^2 = \frac{\lambda + 2\mu}{\rho}\,, \qquad c_s^2 = \frac{\mu}{\rho} \tag{2}$$

where λ and μ are the Lamé constants, and ρ is the mass density.

The Fourier transform of Eq. (1) gives the following frequency domain representation:

$$(c_p^2 - c_s^2)u_{i,ij}(Q,\omega) + c_s^2 u_{j,ii}(Q,\omega) + \omega^2 u_j(Q,\omega) = 0\,. \tag{3}$$

Use of the reciprocal relation for two elastodynamic states of the same angular frequency ω results in the following displacement BIE for a source point P interior to the domain in question:

$$\begin{aligned} \mathcal{U}(P,\omega) \equiv u_k(P,\omega) - \int_{\Gamma_b} \big[U_{kj}(P,Q,\omega)\, t_j(Q,\omega) - T_{kj}(P,Q,\omega)\, u_j(Q,\omega)\big]\,\mathrm{d}Q \\ + \int_{\Gamma_c^+} T_{kj}(P,Q,\omega)\, \Delta u_j(Q,\omega)\,\mathrm{d}Q = 0 \end{aligned} \tag{4}$$

where Q denotes a field point, u_j and t_j are the displacement and traction vectors, respectively, and Δu_j is the displacement jump vector across the crack surfaces. As Δu_j is used as the unknown on the crack, only one crack surface, *e.g.*, Γ_c^+, needs to be discretized.

For P off the boundary, the kernel functions are not singular and it is permissible to differentiate Eq. (4) with respect to P, yielding the displacement gradients. Substitution of these gradients into Hooke's law and then Cauchy's relation results in the following BIE for surface traction:

$$\begin{aligned} \mathcal{T}(P,\omega) \equiv t_k(P,\omega) - n_\ell(P) \int_{\Gamma} \big[D_{kj\ell}(P,Q,\omega)\, t_j(Q,\omega) - S_{kj\ell}(P,Q,\omega)\, u_j(Q,\omega)\big]\,\mathrm{d}Q \\ + n_\ell^+(P) \int_{\Gamma_c^+} S_{kj\ell}(P,Q,\omega)\, \Delta u_j(Q,\omega)\,\mathrm{d}Q = 0 \end{aligned} \tag{5}$$

where n_ℓ is the outward normal vector to the related boundary. It is well known that this traction BIE is essential for treating crack geometries.

The expressions for the elastodynamic kernel tensors $U_{kj}, T_{kj}, D_{kj\ell}$ and $S_{kj\ell}$ in Eqs. (4) and (5) can be found in, *e.g.*, [**17**].

It can be shown that the limits of the integrals in Eqs. (4) and (5) as P approaches the boundary exist. From now on, for $P \in \Gamma$, the BIE is understood in this limiting sense.

The Galerkin boundary integral formulation is obtained by taking the shape functions ψ_m employed in approximating the boundary tractions and displacements as weighting functions for Eqs. (4) and (5). In order to obtain a symmetric coefficient matrix as the name implies, Eq. (4) needs to be employed on Γ_{bu} while Eq. (5) needs to be used on Γ_t, *i.e.*

$$\int_{\Gamma_{bu}} \psi_m(P)\, \mathcal{U}(P,\omega)\, \mathrm{d}P = 0 \tag{6}$$

$$\int_{\Gamma_t} \psi_m(P)\, \mathcal{T}(P,\omega)\, \mathrm{d}P = 0\,. \tag{7}$$

One of the advantages of the frequency-domain analysis is that Eqs. (6) and (7) have a similar form as those in elastostatics. Thus, the reader is referred to, *e.g.*, Reference [**24**] for more details on some aspects of the numerical implementation of these equations.

2.2 - *Treatment of singular integrals*

The main computational task in implementing Eqs. (6) and (7) is the evaluation of the singular integrals. These integrals can be decomposed into two parts as follows:

$$\int\int I\, \mathrm{d}Q\, \mathrm{d}P = \int\int I^s\, \mathrm{d}Q\, \mathrm{d}P + \int\int (I - I^s)\, \mathrm{d}Q\, \mathrm{d}P \tag{8}$$

where I and I^s denote an elastodynamic kernel and its elastostatic counterpart, respectively. It should be noted that I involves modified Bessel functions of the second kind.

As the general procedure for treating the singular and/or hypersingular integrals in the first part $\int\int I^s\, \mathrm{d}Q\, \mathrm{d}P$ has been presented in [**24, 25**], we therefore focus on the second term.

As the distance r between P and Q tends to zero ($\forall \omega > 0$), the modified Bessel functions of the second kind take the following forms:

$$K_0(z) = -\ln \frac{z}{2} - \gamma + \mathcal{O}(z) \tag{9}$$

$$K_1(z) = \frac{1}{z} + \frac{z}{2}\left(\ln\frac{z}{2} + \gamma - \frac{1}{2}\right) + \mathcal{O}(z^2) \tag{10}$$

$$K_2(z) = \frac{1}{z^2} - \frac{1}{2} + \mathcal{O}(z^3) \tag{11}$$

where z could be either $z_1 = i\omega r/c_p$ or $z_2 = i\omega r/c_s$, $i^2 = -1$, $r = \|P - Q\|$ and γ is Euler's constant.

Use of these above equations in the elastodynamic kernels results in the following asymptotic behavior for the kernel functions,

$$U_{kj} - U^s_{kj} = \frac{E_\omega}{2\pi\mu}\,\delta_{kj} = \mathcal{O}(1) \tag{12}$$

$$T_{kj} - T^s_{kj} = \mathcal{O}(r\ln r) \tag{13}$$

$$D_{kj\ell} - D^s_{kj\ell} = \mathcal{O}(r\ln r) \tag{14}$$

$$S_{kj\ell} - S^s_{kj\ell} = \mathcal{O}(\ln r)\,, \tag{15}$$

where δ_{kj} is the Kronecker delta and (ν is Poisson's ratio)

$$E_\omega = \frac{-1}{4(1-\nu)}\left[(3-4\nu)\left(\ln\frac{i\omega}{2} + \gamma\right) + \frac{1}{2}\right] + \frac{1}{2}\left[\ln c_s + \left(\frac{c_s}{c_p}\right)^2 \ln c_p\right]. \tag{16}$$

It can be seen that the second part $\int\int (I - I^s)\,\mathrm{d}Q\,\mathrm{d}P$ is regular except when the integrand is $S_{kj\ell} - S^s_{kj\ell}$. However, this logarithmic singularity can be treated straightforwardly by Gauss quadrature using the following conversion [**26**]:

$$\int_0^1 f(r)\ln r\,\mathrm{d}r = -\int_0^1\int_0^1 f(sr)\,\mathrm{d}s\,\mathrm{d}r\,. \tag{17}$$

Finally, it should be noted that, since both I and I^s are singular, the singular terms in the kernel difference $(I - I^s)$ must be algebraically canceled out to avoid large round-off errors. By doing that, the integrand $(I - I^s)$ can be accurately obtained by using the expression for the elastodynamic kernel I where $K_0(z)$, $K_1(z)$, $K_2(z)$ are replaced by their less significant parts ($\mathcal{O}(z)$, $\mathcal{O}(z^2)$ and $\mathcal{O}(z^3)$, respectively, in Eqs. (9)

through (11)), and $\psi_{,r}$, $\chi_{,r}$, $\psi_{,rr}$, $\chi_{,rr}$ are replaced by $\psi_{,r} - AA$, $\chi_{,r} - AA + BB$, $\psi_{,rr} - CC$, $\chi_{,rr} + DD$, respectively. Here,

$$AA = \frac{z_2^2}{2r}\left(\ln\frac{z_2}{2} + \gamma - \frac{1}{2}\right) \tag{18}$$

$$BB = \left(\frac{c_s}{c_p}\right)^2 \frac{z_1^2}{2r}\left(\ln\frac{z_1}{2} + \gamma - \frac{1}{2}\right) \tag{19}$$

$$CC = \left[\left(\frac{c_s}{c_p}\right)^2 \frac{z_1^2}{2}\left(\ln\frac{z_1}{2} + \gamma - \frac{1}{2}\right) + \frac{z_2^2}{2}\right]\frac{1}{r^2} \tag{20}$$

$$DD = \left[-\left(\frac{c_s}{c_p}\right)^2 \frac{z_1^2}{2}\left(\ln\frac{z_1}{2} + \gamma - \frac{3}{2}\right) + \frac{z_2^2}{2}\left(\ln\frac{z_2}{2} + \gamma - \frac{3}{2}\right)\right]\frac{1}{r^2}\,. \tag{21}$$

3 - Dynamic T-stress

An exact boundary integral formula for the DTS is derived in this section for cracks of arbitrary geometry. The formula is based upon the series expansion for the stress field in the vicinity of a crack tip [**22**] (Fig. 2)

$$\sigma_{ij}(r,\phi) = \frac{K_{\mathrm{I}}}{\sqrt{2\pi r}} f_{ij}^{\mathrm{I}}(\phi) + \frac{K_{\mathrm{II}}}{\sqrt{2\pi r}} f_{ij}^{\mathrm{II}}(\phi) + T\,\delta_{1i}\delta_{1j} + \mathcal{O}(r^{1/2}) \tag{22}$$

where K_{I} and K_{II} are the mode-I and mode-II SIFs, and f_{ij}^{I} and f_{ij}^{II} are universal functions of angle ϕ.

For $\phi = 0$, one gets

$$\begin{Bmatrix} \sigma_{11}(r,0) \\ \sigma_{22}(r,0) \end{Bmatrix} = \frac{1}{\sqrt{2\pi r}} \begin{Bmatrix} K_{\mathrm{I}} \\ K_{\mathrm{I}} \end{Bmatrix} + \begin{Bmatrix} T \\ 0 \end{Bmatrix} + \mathcal{O}(r^{1/2}) \tag{23}$$

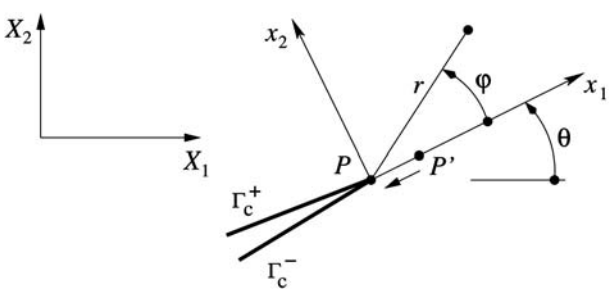

Fig. 2. Global coordinate system X_1X_2 and crack tip coordinate system x_1x_2.

which results in the following expression for evaluating the T-stress:

$$T = \lim_{r\to 0}\Big[\sigma_{11}(r,0) - \sigma_{22}(r,0)\Big]\,. \tag{24}$$

The Fourier transform of this equation yields the following expression for the T-stress in the frequency domain:

$$T(\omega) = \lim_{r\to 0}\Big[\sigma_{11}(r,0,\omega) - \sigma_{22}(r,0,\omega)\Big]\,. \tag{25}$$

Consider an interior point P' ahead of a crack tip P and in the direction of $\phi = 0$ as shown in Fig. 2. In this work, Eq. (25) is evaluated using the BIE for the stress components at P' (see Eq. (5)) and a limit process is carried out as P' tends to the crack tip P ($r \to 0$),

$$\begin{aligned}\sigma_{k\ell}(P,\omega) = &\int_{\Gamma_b}\Big[D_{k\ell j}(P,Q,\omega)\,t_j(Q,\omega) - S_{k\ell j}(P,Q,\omega)\,u_j(Q,\omega)\Big]\mathrm{d}Q\\ &- \lim_{P'\to P}\int_{\Gamma_c^+} S_{k\ell j}(P',Q,\omega)\,\Delta u_j(Q,\omega)\,\mathrm{d}Q\,.\end{aligned} \tag{26}$$

Use of Eq. (26) in Eq. (25) results in

$$\begin{aligned}T(\omega) = &\int_{\Gamma_b}\Big[\Delta D_k(P,Q,\omega)\,t_k(Q,\omega) + \Delta S_k(P,Q,\omega)\,u_k(Q,\omega)\Big]\mathrm{d}Q\\ &+ \lim_{P'\to P}\int_{\Gamma_c^+}\Delta S_k(P',Q,\omega)\,\Delta u_k(Q,\omega)\,\mathrm{d}Q\end{aligned} \tag{27}$$

where $\Delta D_k = D_{11k} - D_{22k}$ and $\Delta S_k = S_{22k} - S_{11k}$.

For all $\omega > 0$ and as $P' \to P$, the second integral in Eq. (26) tends to infinity (the stress field $\sigma_{k\ell}$ is known to be singular at crack tips) whereas the second integral in Eq. (27) should be bounded as T-stress is a non-singular term. In fact, by using relation (15), Eq. (27) can be rewritten as

$$\begin{aligned}T(\omega) = &\int_{\Gamma_b}\Big[\Delta D_k(P,Q,\omega)\,t_k(Q,\omega) + \Delta S_k(P,Q,\omega)\,u_k(Q,\omega)\Big]\mathrm{d}Q\\ &+ \lim_{P'\to P}\int_{\Gamma_c^+}\Delta S_k^s(P',Q)\,\Delta u_k(Q)\,\mathrm{d}Q\\ &+ \lim_{P'\to P}\int_{\Gamma_c^+}\Big[\Delta S_k(P',Q,\omega) - \Delta S_k^s(P',Q)\Big]\,\Delta u_k(Q,\omega)\,\mathrm{d}Q\,.\end{aligned} \tag{28}$$

If this equation is discretized, the only limits that need to be taken care of are those associated with the crack-tip element. Let these limits be denoted as T_{ct}, we have

$$
\begin{aligned}
T_{ct} = & \lim_{P' \to P} \int_{\Gamma_{ct}^{+}} \Delta S_k^s(P', Q)\, \Delta u_k(Q)\, \mathrm{d}Q \\
& + \lim_{P' \to P} \int_{\Gamma_{ct}^{+}} \left[\Delta S_k(P', Q, \omega) - \Delta S_k^s(P', Q) \right] \Delta u_k(Q, \omega)\, \mathrm{d}Q
\end{aligned} \tag{29}
$$

where Γ_{ct}^{+} is part of the Γ_c^{+} discretized by the crack-tip element.

By numerically implementing this equation using a standard quadratic element, as proven in [**6**], the first integral on the right hand side is continuous as $P' \to P$. The second limit in Eq. (29) should also be bounded as its integrand is only weakly singular as discussed in Section 2.2. In other words, the limit processes in Eq. (29) are not necessary and the two integrals in this equation can be directly evaluated at the crack tip ($P' \equiv P$).

4 - Dynamic biaxiality ratio

The biaxiality ratio B, proposed by Leevers and Radon [**23**], is a dimensionless quantity and defined as

$$B = \frac{T\sqrt{\pi a}}{K_{\mathrm{I}}} \tag{30}$$

where K_{I} is the mode-I SIF and a is the crack length.

For dynamic analysis of cracks, the same concept can be adopted to define the DBR $B(t)$ given by

$$B(t) = \frac{T(t)\sqrt{\pi a}}{K_{\mathrm{I}}(t)} \tag{31}$$

where $K_{\mathrm{I}}(t)$ is the time history of the mode-I DSIF.

There are several available approaches for numerically evaluating the SIFs. Among these methods, the displacement correlation technique (DCT) based upon the displacement jump in the vicinity of the crack tip is one of most effective. Details of using this technique to obtain the time history of the mode-I and mode-II DSIFs can be found in, *e.g.*, [**17**]. A brief review is given as follows: For stationary cracks (as those considered in this work), the frequency-domain mode-I SIF is given by

$$K_{\mathrm{I}}(\omega) = \frac{\mu}{4(1-\nu)} \lim_{r \to 0} \sqrt{\frac{2\pi}{r}}\, \Delta u_n(\omega) \tag{32}$$

where Δu_n is the normal component of the displacement jump vector, and r is the distance to the crack tip.

The dynamic analysis of cracks reported in this work is performed using the MQP element developed in [**28**]. By using the MQP shape functions in Eq. (32), the mode-I SIF can simply and accurately be obtained as

$$K_{\mathrm{I}}(\omega) = \frac{\mu}{12(1-\nu)}\sqrt{\frac{2\pi}{L}}\left(8\Delta u_n^{(2)} - \Delta u_n^{(3)}\right) \tag{33}$$

where L is the distance between the two end-nodes, and the superscripts (2) and (3) denote the quarter-point node and non-tip end-node of the crack-tip element, respectively.

As K_{I} is directly given in terms of the nodal values of the displacement jump of the crack-tip element, and the MQP element enhances the accuracy of the nodal displacement jump [**28**], this enhances the accuracy of the obtained frequency response $K_{\mathrm{I}}(\omega)$ [**16**].

At this point, IFFT can be employed (see, *e.g.*, [**17**]) to convert $T(\omega)$ in Eq. (28) and $K_{\mathrm{I}}(\omega)$ in Eq. (33) to $T(t)$ and $K_{\mathrm{I}}(t)$, respectively. These transient parameters are required for determining the dynamic biaxiality ratio $B(t)$ as seen in Eq. (31). For more details of this frequency-to-time conversion, the reader is referred to, *e.g.*, [**15**] or [**17**].

5 - Test examples

Four numerical examples involving viscoelastic materials under impact loading are given in this section to illustrate the accuracy and effectiveness of the proposed BIE (28) when it comes to evaluating the DTS and DBR. The type of impact loading considered in these examples is the Heaviside step function $\sigma_0 H(t)$ as shown in Fig. 3. Note for this type of function that an unloading needs to take place well before the end of the analysis period in order to create an impact situation. The internal damping of the viscoelastic materials is considered by means of a complex shear modulus defined as $\mu_c = \mu(1 + 2i\zeta)$ where ζ is the damping ratio. The following material properties and damping ratio are employed for all the test examples: $\mu = 76.923$ GPa, $\nu = 0.3$, $\rho = 5,000$ kg/m^3, and $\zeta = 1\%$. Undamped cases are not considered here as their transient responses never decay which violates the periodic nature of the standard FFT and IFFT algorithm discussed in Section 4. This explains why spurious oscillations were observed in the time solution for cases with zero damping ratio [**15, 10**]. Note that the referenced numerical results, employed in this paper for the purpose of comparison, are digitized data.

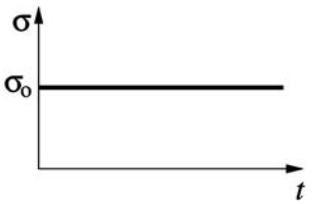

Fig. 3. Heaviside step loading.

5.1 - *Dynamic T-stress for a mode-I crack in a finite plate*

The first two examples involve a mode-I crack of length $2a = 4.8$ mm in a finite plate of size $(2H \times 2B) = (20 \text{ mm} \times 40 \text{ mm})$ as shown in Fig. 4. The plate is subjected to a uniaxial tension $\sigma(t) = \sigma_0 H(t)$ depicted in Fig. 3. Note that the geometry and material data employed here are adopted from Ref. [**9**] for the purpose of comparing our results with other numerical solutions available in the literature.

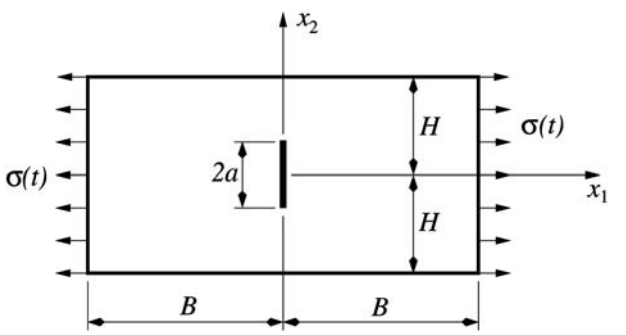

Fig. 4. A plate with a centrally located mode-I crack.

Based on a convergence study, a total of 20 elements is employed on the boundary and 10 uniform elements are used to discretize the crack. For the frequency response analysis of the DTS, another convergence study reveals that a frequency step $\Delta f = 0.001$ MHz and a number of samplings $N = 2^{11} = 2,048$ are needed. This results in a Nyquist frequency f_{Nyq} of 1.024 MHz. Figure 5 depicts the conjugate symmetry about f_{Nyq} for the frequency response $T_1(\omega)$ of the DTS (due to a unit Heaviside step loading $\sigma(t) = H(t)$) obtained by using Eq. (28). According to this figure, the chosen value for f_{Nyq} is justified as there is no significant peak for frequencies larger than 1.024 MHz.

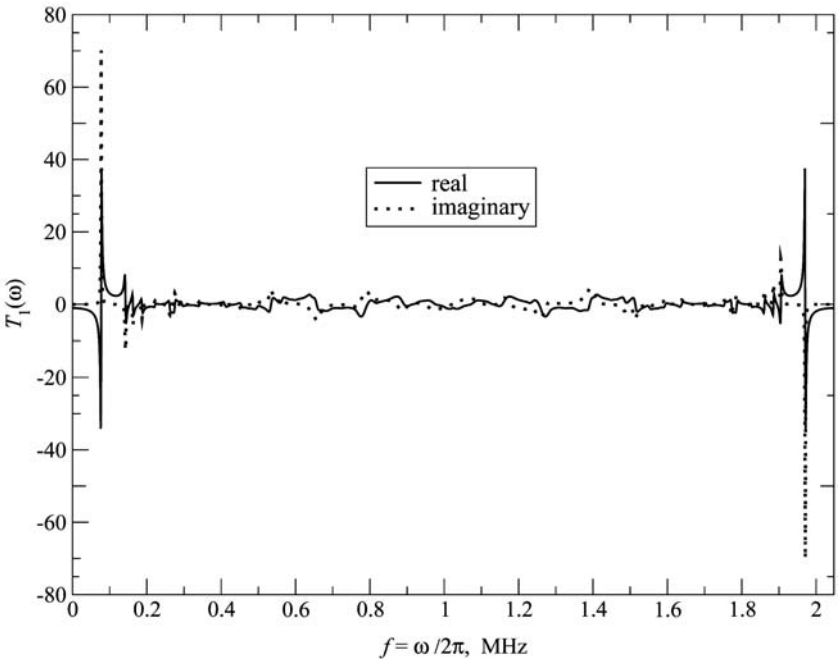

Fig. 5. Frequency response $T_1(\omega)$ ($\theta = 0$ and $\zeta = 1\%$).

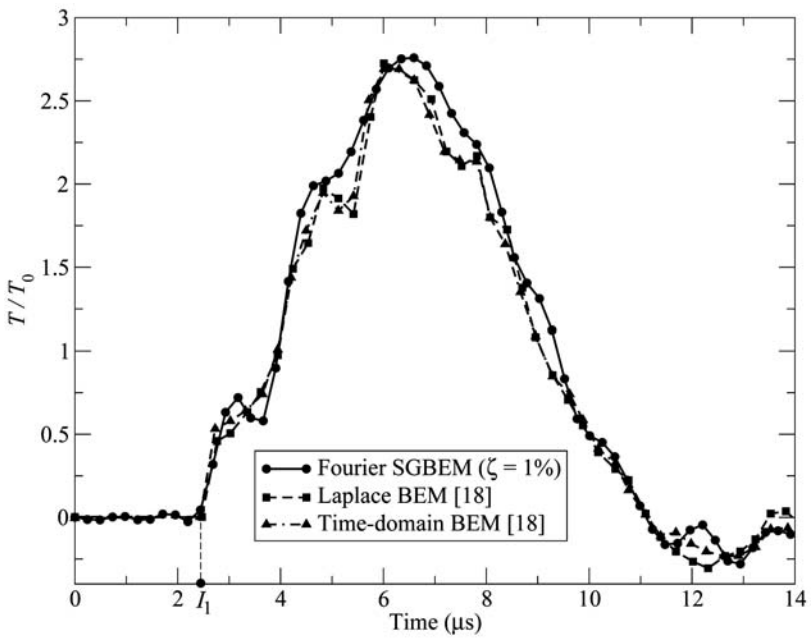

Fig. 6. Normalized DTS under Heaviside step loading ($\theta = 0$ and $\zeta = 1\%$).

By applying the FFT to $\sigma_0 H(t)$ and IFFT to the frequency response $T_1(\omega)$, the transient response $T(t)$ can be found. Here, the DTS is normalized by the corresponding static T-stress T_0 (the T-stress for the same problem, but under a constant tension σ_0). For the sake of comparison, the value of T_0 reported in [**18**] ($T_0 = -1.058\,\sigma_0$) is also used here. Figure 6 shows that the time history of the normalized DTS T/T_0 obtained from this work agrees very well with those reported in [**18**] using the BEM and interaction M-integral method. Of particular importance is the fact that the SGBEM curve shows similar oscillations caused by various scattered waves as on the two BEM curves. Specifically, the SGBEM and BEM solutions agree on the time needed for the incident longitudinal wave to travel from the vertical edges of the plate to the crack ($I_1 \simeq 2.5\,\mu$s).

Finally, it should be noted that the resolution of the SGBEM curve seen in Fig. 6 was doubled using a very simple interpolation technique available with the FFT (see, *e.g.*, [**27**]).

5.2 - *Dynamic biaxiality ratio for a mode-I crack in a finite plate*

The numerical result for the DBR $B(t)$ for the mode-I crack problem described in Section 5.1 is given next. Toward this end, it is necessary to obtain the mode-I DSIF first, using the technique proposed in [**17**] and summarized in Section 4. As expected,

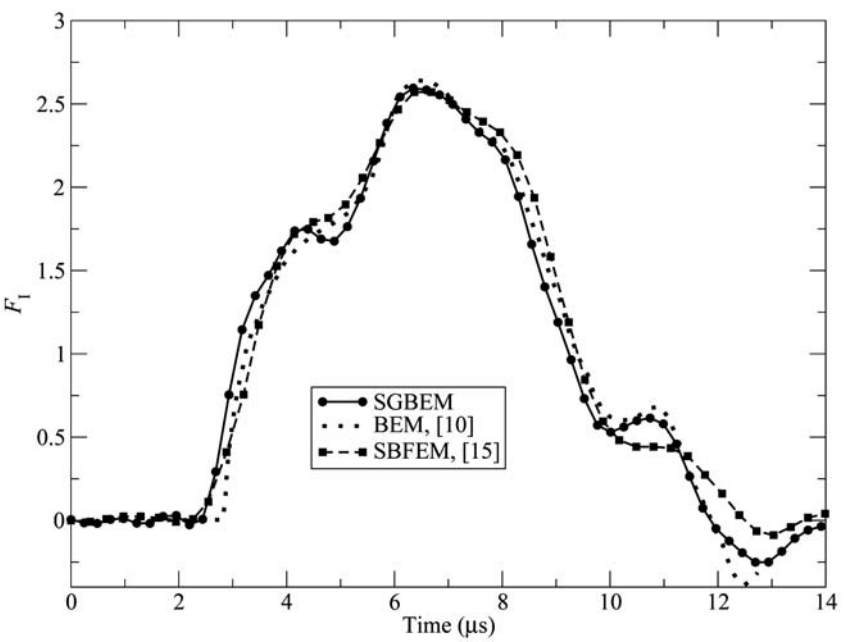

Fig. 7. F_1 under Heaviside step loading ($\theta = 0$ and $\zeta = 1\%$).

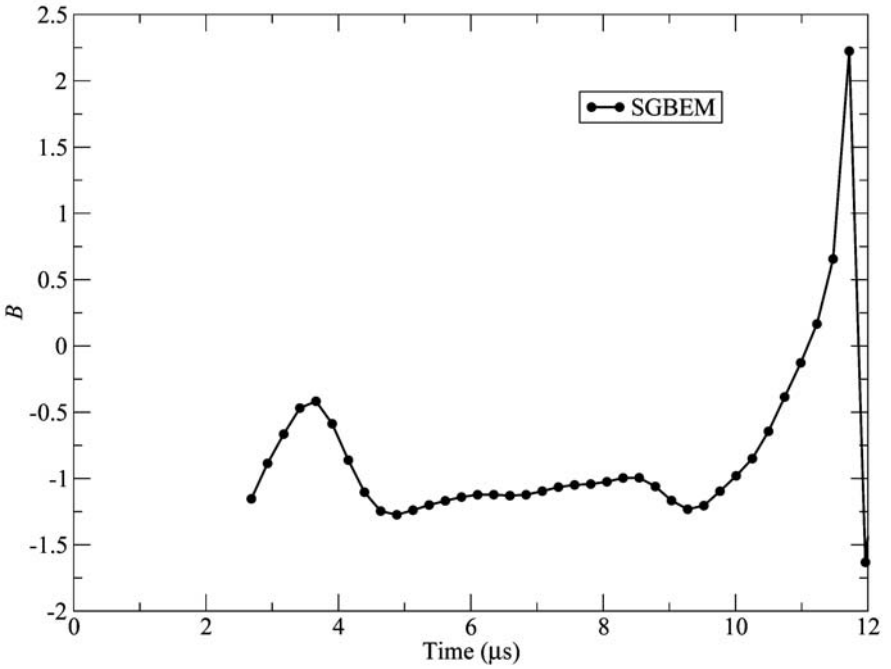

Fig. 8. Dynamic B under Heaviside step loading ($\theta = 0$ and $\zeta = 1\%$).

the same frequency step and sampling number are employed to convert $K_{\mathrm{I}}(\omega)$ to $K_{\mathrm{I}}(t)$. Figure 7 depicts some numerical results for the normalized mode-I DSIF, defined as $F_{\mathrm{I}} = \dfrac{K_{\mathrm{I}}}{\sigma_o\sqrt{\pi a}}$. As reported in [**17**] and seen in Fig. 7, there is a very good agreement between the SGBEM F_{I} solution and those obtained from finite difference method [**9**], BEM [**10**], SBFEM [**15**], *etc.*

Finally, the DBR $B(t)$ can be found (see Fig. 8) by using the DTS solution $T(t)$ (mentioned in Section 5.1) and the above $K_{\mathrm{I}}(t)$ in Eq. (31). Note that $B(t)$ is not available before I_1 as both $T(t)$ and $K_{\mathrm{I}}(t)$ are supposed to be zero during that time. To the best knowledge of the authors, no reference is available in the literature to be compared with the result shown in Fig. 8.

5.3 - *Dynamic T-stress for a mixed-mode crack in a finite plate*

The last two test examples deal with a mixed-mode crack in a finite plate under a uniaxial tension $\sigma(t) = \sigma_0 H(t)$ (see Fig. 9). The crack has an orientation $\theta = 45^\circ$ relative to the direction of the load and a length $2a = 10\sqrt{10}$ mm. The size of the plate is $(2H \times 2B) = (30\ \text{mm} \times 60\ \text{mm})$.

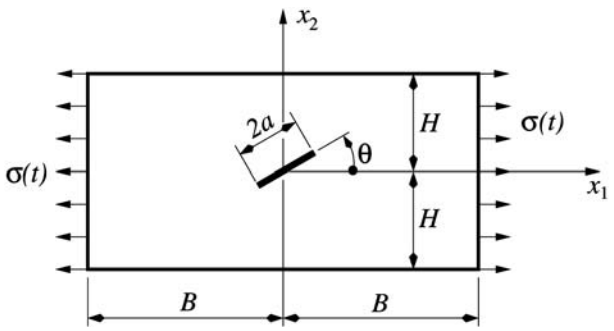

Fig. 9. A plate with a centrally located mixed-mode crack.

Based on a convergence study, a total of 20 elements is employed on the boundary and 10 uniform elements are used to discretize the crack. For the frequency response analysis of the DTS, a frequency step $\Delta f = 500$ Hz and a number of samplings $N = 2^{12} = 4,096$ need to be selected. Figure 10 shows the frequency response $T_1(\omega)$ while Fig. 11 depicts the normalized T/T_0 curves where T_0 is adopted from Reference [18] ($T_0 = -1.058\,\sigma_0$) for the purpose of comparison. It can be seen from

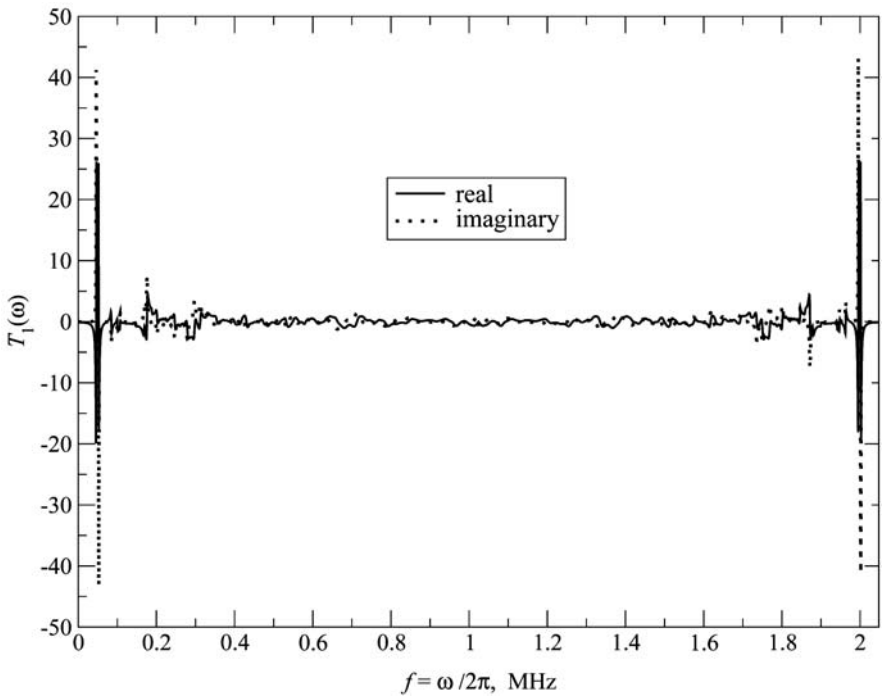

Fig. 10. Frequency response $T_1(\omega)$ ($\theta = 45^\circ$ and $\zeta = 1\%$).

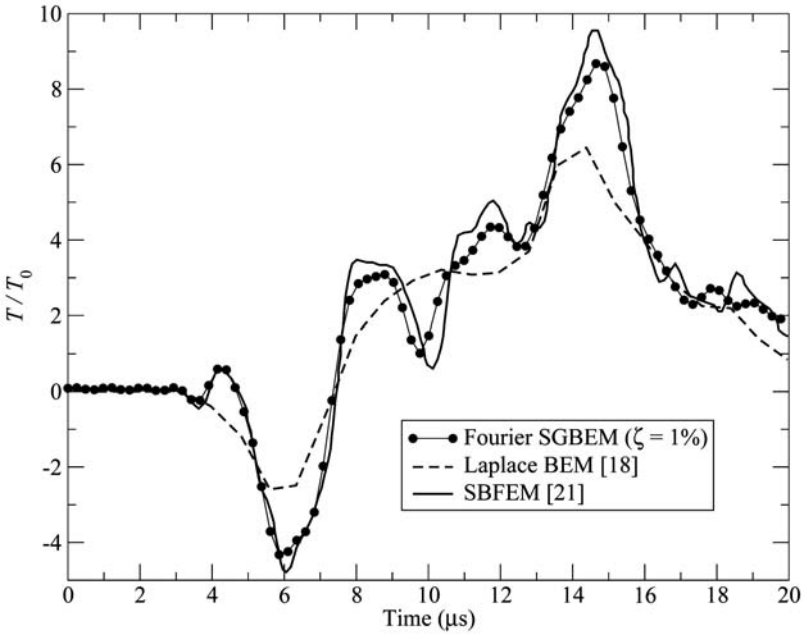

Fig. 11. F_{I} under Heaviside step loading ($\theta = 45^{\circ}$ and $\zeta = 1\%$).

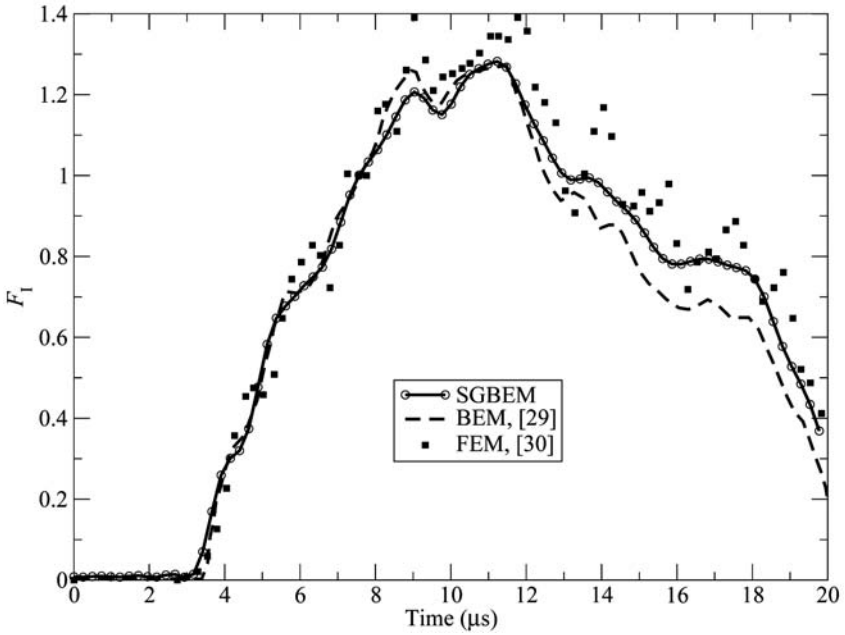

Fig. 12. F_{I} under Heaviside step loading ($\theta = 45^{\circ}$ and $\zeta = 1\%$).

Fig. 11 that while the SGBEM solution does not agree with the BEM [**18**] one, there is a very good agreement between the SGBEM and SBFEM [**21**] curves.

5.4 - *Dynamic biaxiality ratio for a mixed-mode crack in a finite plate*

The same approach, as described in Section 5.2, is employed here to evaluate the DBR $B(t)$ for the mixed-mode crack problem under consideration. Although there is no available reference to assess the accuracy of the DBR time history shown in Fig. 13, this SGBEM result can be justified as both the related DTS (Fig. 11) and mode-I DSIF (Fig. 12) agree well with some referenced solutions. In fact, for the normalized mode-I DSIF, a good agreement between the SGBEM, BEM [**29**] and FEM [**30**] results can be observed in Fig. 12.

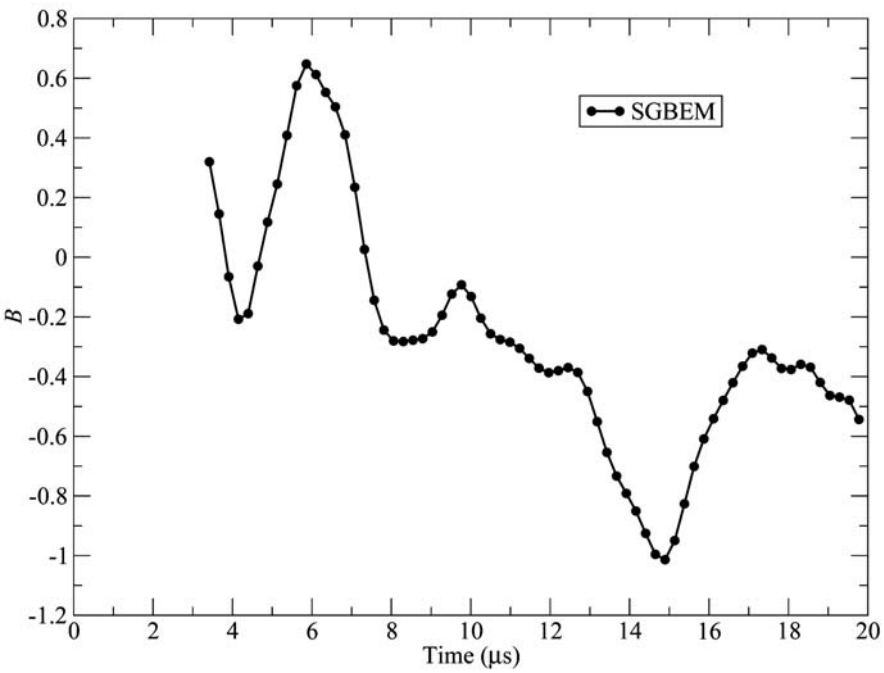

Fig. 13. Dynamic B under Heaviside step loading ($\theta = 45^\circ$ and $\zeta = 1\%$).

6 - Conclusion

In this paper, a weakly singular 2-D BIE in the frequency domain was developed for numerically calculating the frequency response of the DTS in the post-processing

stage of a frequency-domain boundary element analysis of stationary cracks under dynamic loading conditions. The transient response of the DTS can easily be obtained by applying the IFFT to its frequency response. This BIE is simpler than those used to determine the stress components at an interior point to a domain. It can be employed at the crack tip to accurately evaluate the DTS without any concern about the numerical sensitivity of the result. The technique is much more computationally effective than the M-integral method as the latter requires evaluating both the stress and displacement at several interior points used as Gauss integration points.

For the test examples considered in this work, the numerical results for the DTS agree very well with a few referenced solutions available in the literature. Although these comparisons cannot be used to judge the accuracy of the BIE developed, at least they have helped to validate the proposed technique.

Acknowledgments. This research was partially supported by the NSF Grant CMMI-0653796 and the NASA Grant NNM07AA09A-03.

References

[1] J. G. Williams and P. D. Ewing, *Fracture under complex stress – The angled crack problem*, Internat. J. Fracture 8 (1972), 441-446.

[2] Y. Ueda, K. Ikeda, T. Yao and M. Aoki, *Characteristics of brittle fracture under general combined modes including those under bi-axial tensile loads*, Engrg. Fracture Mech. **18** (1983), 1131-1158.

[3] M. R. Ayatollahi, M. J. Pavier and D. J. Smith, *Determination of T-stress from finite element analysis for mode I and mixed mode I/II loading*, Internat. J. Fracture **91** (1998), 283-298.

[4] G. H. Paulino and J.-H. Kim, *A new approach to compute T-stress in functionally graded materials by means of the interaction integral method*, Engrg. Fracture Mech. **71** (2004), 1907-1950.

[5] B. Yang and K. Ravi-Chandar, *Evaluation of elastic T-stress by the stress difference method*, Engrg. Fracture Mech. **64** (1999), 589-605.

[6] A.-V. Phan, *A non-singular boundary integral formula for determining the T-stress for cracks of arbitrary geometry*, (under review).

[7] A. Sutradhar and G. H. Paulino, *Symmetric Galerkin boundary element computation of T-stress and stress intensity factors for mixed-mode cracks by the interaction integral method*, Eng. Anal. Bound. Elem. **28** (2004), 1335-1350.

[8] Y. Z. Chen, *Closed form solutions of T-stress in plane elasticity crack problems*, Internat. J. Solids Structures **37** (2000), 1629-1637.

[9] Y. M. CHEN, *Numerical computation of dynamic stress intensity factors by a Lagrangian finite-difference method (the HEMP code)*, Engrg. Fracture Mech. **7** (1975), 653-660.

[10] F. CHIRINO and J. DOMINGUEZ, *Dynamic analysis of cracks using boundary element method*, Engrg. Fracture Mech. **34** (1989), 1051-1061.

[11] F. CHIRINO, R. GALLEGO, A. SÁEZ and J. DOMINGUEZ, *A comparative study of three boundary element approaches to transient dynamic crack problems*, Eng. Anal. Bound. Elem. **13** (1994), 11-19.

[12] P. FEDELINSKI, M. H. ALIABADI and D. P. ROOKE, *The Laplace transform DBEM for mixed-mode dynamic crack analysis*, Computers & Structures **59** (1996), 1021-1031.

[13] M. P. ARIZA and J. DOMINGUEZ, *General BE approach for three-dimensional dynamic fracture analysis*, Eng. Anal. Bound. Elem. **26** (2002), 639-651.

[14] S. H. SONG and G. H. PAULINO, *Dynamic stress intensity factors for homogeneous and smoothly heterogeneous materials using the interaction integral method*, Internat. J. Solids Structures **43** (2006), 4830-4866.

[15] Z. J. YANG, A. J. DEEKS and H. HAO, *Transient dynamic fracture analysis using scaled boundary finite element method: a frequency-domain approach*, Engrg. Fracture Mech. **74** (2007), 669-687.

[16] A.-V. PHAN, L. J. GRAY and A. SALVADORI, *Symmetric-Galerkin boundary element analysis of the dynamic stress intensity factors in the frequency domain*, Mech. Res. Comm. **37** (2010), 177-183.

[17] A.-V. PHAN, L. J. GRAY and A. SALVADORI, *Transient analysis of the dynamic stress intensity factors using SGBEM for frequency-domain elastodynamics*, Comput. Methods Appl. Mech. Engrg. **199** (2010), 3039-3050.

[18] J. SLADEK, V. SLADEK and P. FEDELINSKI, *Computation of the second fracture parameter in elastodynamics by the boundary element method*, Advances in Engineering Software **30** (1999), 725-734.

[19] K. R. JAYADEVAN, R. NARASIMHAN, T. S. RAMAMURTHY and B. DATTAGURU, *A numerical study of T-stress in dynamically loaded fracture specimens*, Internat. J. Solids Structures **38** (2001), 4987-5005.

[20] D. K. SHIN and J. J. LEE, *Numerical analysis of dynamic T stress of moving interfacial crack*, Internat. J. Fracture **119** (2003), 223-245.

[21] C. SONG and Z. VRCELJ, *Evaluation of dynamic stress intensity factors and T-stress using the scaled boundary finite-element method*, Engrg. Fracture Mech. **75** (2008), 1960-1980.

[22] M. L. WILLIAMS, *On the stress distribution at the base of a stationary crack*, J. Appl. Mech. **24** (1957), 109-114.

[23] P. S. LEEVERS and J. C. RADON, *Inherent stress biaxiality in various fracture specimen geometries*, Internat. J. Fracture **19** (1982), 311-325.

[24] A. SUTRADHAR, G. H. PAULINO and L. J. GRAY, *Symmetric Galerkin boundary element method*, Springer-Verlag, Berlin 2008.

[25] L. J. GRAY, *Evaluation of singular and hypersingular Galerkin boundary integrals: direct limits and symbolic computation*. In: Singular Integrals in the Boundary Element Method. Advances in Boundary Elements, V. Sladek and J. Sladek, eds., Computational Mechanics Publishers, 1998, 33-84.

[**26**] B. DANLOY, *Numerical construction of Gaussian quadrature formulas for* $\int_0^1 (-\mathrm{Log}x)\cdot x^{\alpha}\cdot f(x)\cdot dx$ *and* $\int_0^{\infty} E_m(x)\cdot f(x)\cdot dx$, Math. Comp. **27** (1973), 861-869.

[**27**] E. O. BRIGHAM, *The fast Fourier transform and its applications*, Prentice Hall, New Jersey 1988.

[**28**] L. J. GRAY, A.-V. PHAN, G. H. PAULINO and T. KAPLAN, *Improved quarter-point crack tip element*, Engrg. Fracture Mech. **70** (2003), 269-283.

[**29**] J. DOMINGUEZ and R. GALLEGO, *Time domain boundary element method for dynamic stress intensity factor computations*, Internat. J. Numer. Methods Engrg. **33** (1992), 635-647.

[**30**] V. MURTI and S. VALLIAPPAN, *The use of quarter point element in dynamic crack analysis*, Engrg. Fracture Mech. **23** (1986), 585-614.

ANH-VU PHAN, VAMSI GUDURU
University of South Alabama
307 University Blvd
Mobile, Alabama 36688-0002, USA
e-mail: vphan@jaguar1.usouthal.edu
e-mail: vg703@jaguar1.usouthal.edu